In vivo three-photon imaging of activity of GCaMP6-labeled neurons deep in intact mouse brain

Dimitre G Ouzounov[1,5], Tianyu Wang[1,5], Mengran Wang[1], Danielle D Feng[2], Nicholas G Horton[1], Jean C Cruz-Hernández[2], Yu-Ting Cheng[2], Jacob Reimer[3], Andreas S Tolias[3,4], Nozomi Nishimura[2] & Chris Xu[1]

High-resolution optical imaging is critical to understanding brain function. We demonstrate that three-photon microscopy at 1,300-nm excitation enables functional imaging of GCaMP6s-labeled neurons beyond the depth limit of two-photon microscopy. We record spontaneous activity from up to 150 neurons in the hippocampal stratum pyramidale at ~1-mm depth within an intact mouse brain. Our method creates opportunities for noninvasive recording of neuronal activity with high spatial and temporal resolution deep within scattering brain tissues.

Optical imaging provides the high spatial resolution necessary to resolve individual neurons and neuronal processes, but wide-field images acquired deep within scattering biological tissues are blurred. Multiphoton microscopy (MPM) has substantially extended the penetration depth of high-resolution optical imaging[1,2]. When combined with activity-sensitive fluorescent indicators, MPM enables functional imaging of populations of neurons in their native environment. While two-photon microscopy (2PM) has been successful in recording neuronal activities within the cortex[3–7] of mouse brain, 2PM imaging of subcortical neurons currently requires invasive procedures that either remove overlying brain tissue[8] or insert penetrating optical elements[9–11].

The imaging depth for MPM in scattering biological tissue is limited by the signal-to-background ratio (SBR)[12,13]. When the SBR approaches 1, the image contrast is substantially degraded. For *in vivo* 2PM imaging in densely labeled mouse cortex, the image contrast is lost at depth of 1 mm (refs. 13–16). Because of its higher order of nonlinear excitation and weaker scattering at longer excitation wavelengths, three-photon microscopy (3PM) reduces out-of-focus excitation and has an SBR orders of magnitude higher than that of 2PM at the same depth[17].

The optimal wavelengths[18–20] for minimum excitation attenuation in mouse brain tissue occur at two narrow regions centered at 1,300 nm and 1,700 nm (ref. 17). 3PM at the 1,300-nm spectral window enables three-photon excitation (3PE) of a variety of blue and green fluorophores, such as the current generations of protein-based genetically encoded calcium indicators (GECIs; e.g., GCaMP6 (ref. 21)), for which researchers have found increasingly broader applications in neuroscience research.

Here, we demonstrate that 3PM at 1,300-nm excitation in combination with GCaMP6s[21] is capable of structural and functional imaging of populations of neurons as deep as the SP layer of the CA1 hippocampal region within intact mouse brains. The demonstrated method will introduce potential applications where noninvasive, high spatial- and temporal-resolution imaging deep within tissue is required.

We used a custom-built multiphoton microscope as well as a noncolinear optical parametric amplifier (NOPA) and a mode-locked Ti:sapphire laser for 3PM and 2PM, respectively (**Supplementary Fig. 1a–c**).

To validate functional imaging with 3PM, we compared it with 2PM, which is capable of detecting single action potentials[21]. We used a time-division multiplexing (TDM) scheme (**Supplementary Fig. 1d**), which enabled us to alternatively image neuronal activity using 2PM (at 920 nm) and 3PM (at 1300 nm) within ~1 μs of each other. We recorded activity in cortical layer 2/3 (L2/3) neurons in a transgenic mouse (CamKII-tTA/tetO-GCaMP6s) (**Fig. 1a,b**). Neuronal activity traces recorded by 2PM and 3PM were essentially the same, with a Pearson's correlation coefficient of 0.976 ± 0.004 (mean ± s.e.m.) calculated from four neurons over a total of 19 traces (each 75 s long).

Although the SBR of 2PM is adequate for sparsely labeled samples or in shallow regions, many experiments require densely labeled brain tissue—for example, while recording the activities from a large number of neurons simultaneously at multiple depths of a cortical column. We compared 2PM and 3PM SBR by imaging densely labeled vasculature and neurons in deep mouse cortex at the same site and time. For fluorescein-labeled vasculature in an 11-week-old C57BL/6J mouse, SBR approached ~1 for 2PM at 780 μm (**Fig. 1c,d**). In comparison, the SBR for 3PM at the same imaging depth was above 40. In densely labeled transgenic mice (CamKII-tTA/tetO-GCaMP6s, 20 weeks) it is difficult to identify neurons of average brightness using 2PM at the depth of 780 μm (**Fig. 1e,f**). The 3PM image has better contrast, and more neurons are visible in the same field of view (FOV). These results show the
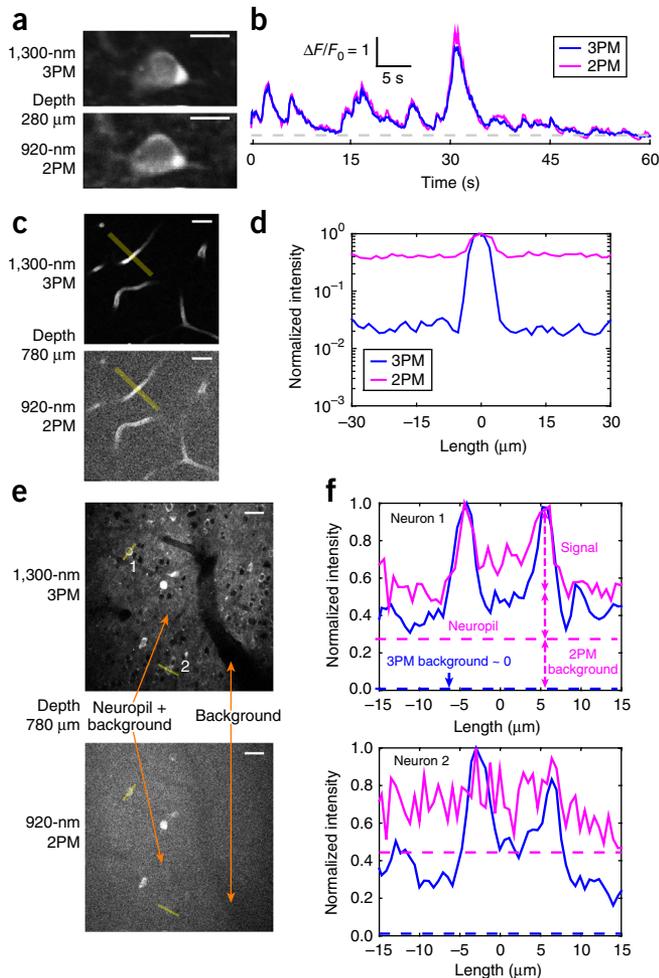
Figure 1 | Comparison of 2PM at 920 nm and 3PM at 1,300 nm for *in vivo* mouse brain imaging. (**a**) Near-simultaneous 2P and 3P imaging of a GCaMP6s-labeled L2/3 neuron in transgenic mouse (CamKII-tTA/tetO-GCaMP6s) cortex located 280 μm below the dura. Scale bars, 10 μm. (**b**) Activity traces of the neuron in **a**. The traces are representative of 19 recordings. (**c**) Measurement of signal-to-background ratio (SBR) of 2PM and 3PM by imaging fluorescein-labeled blood vessel 780 μm deep in mouse cortex (wild type, C57BL/6J). The two images have comparable numbers of signal photons, and they were displayed with the same contrast setting (top 0.2% saturation). Scale bars, 30 μm. (**d**) Quantitative comparison of SBR of blood vessels in **c**. Intensity profiles are drawn along the light yellow lines in **c**, averaged over 7.2-μm line thickness. SBR of 2PM approaches 1 at 780 μm depth, and SBR of 3PM is one to two orders of magnitude higher. The line profile represents similar measurements done on eight blood vessel sections from 720 to 780 μm in depth. (**e**) Measurement of SBR of 2PM and 3PM by imaging GCaMP6s-labeled neurons 780 μm deep in transgenic mouse cortex (CamKII-tTA/tetO-GCaMP6s). The out-of-focus fluorescence is measured inside a blood vessel, which is indicated by the "Background" arrow. Neuropil and the out-of-focus background are indicated by the "Neuropil + Background" arrow. The two images have comparable number of signal photons, and were displayed with the same contrast settings (top 0.4% saturation). Scale bars, 30 μm. (**f**) Quantitative comparison of SBR and neuropil of two neurons in **e**. Intensity profiles are drawn along the light yellow lines in **e**, averaged over 3.5-μm line thickness. The line profiles represent similar measurement done on 20 neurons from 720 to 780 μm in depth.

advantages of the larger SBR of long-wavelength 3PM in densely labeled tissues; in fact, SBR does not limit 3PM imaging capability until much deeper layers[17].
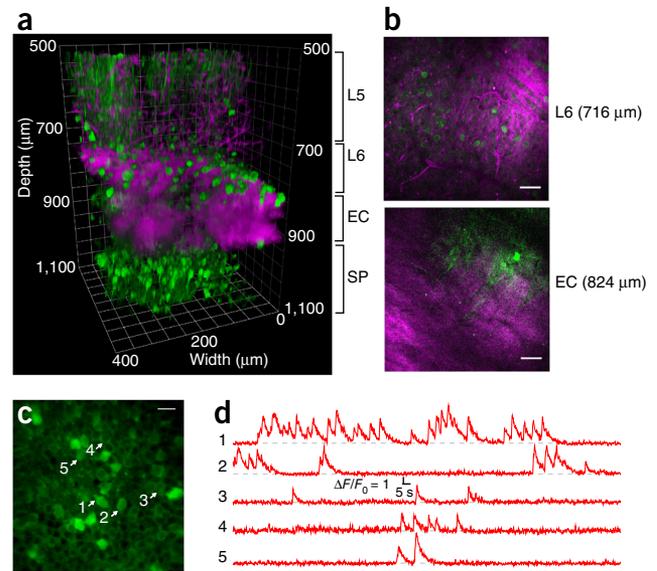
Figure 2 | 3PM of spontaneous activity in neuronal population labeled with GCaMP6s in the SP layer of the CA1 region of the mouse hippocampus. (**a**) 3D reconstruction of 3PM images of GCaMP6s-labeled neurons in the mouse cortex and the hippocampus (green, fluorescence; magenta, THG.). See **Supplementary Video 1** for individual XY frames of the z-stack. (**b**) Selected XY frames at various depths in **a**. THG visualizes blood vessels and myelinated axons (green, fluorescence; magenta, THG). Scale bars, 50 μm. (**c**) Activity recording site in the SP layer of the hippocampus located at 984 μm beneath the dura with a field-of-view of 200 × 200 μm. Scale bar, 20 μm. (**d**) Spontaneous activity recorded from the labeled neurons indicated in **c**. Additional traces from 30 active neurons are shown in **Supplementary Figures 2–4** and **Supplementary Video 2**. The structural and functional imaging in this figure is representative of data from five animals.

We performed 3PM of both the structure and activity of neurons in the SP layer of the mouse hippocampus (**Fig. 2** and **Supplementary Figs. 2–6**). The hippocampal neurons were infected by AAV virus expressing GCaMP6s (synapsin promoter, AAV2/1 encapsulation) in wild-type mice (C57BL/6J). The imaging took place in the third to fifth week after injection (11–16-weeks-old mice). For structural imaging, we acquired a stack from 500 to 1,100 μm (3D reconstruction in **Fig. 2a** and **Supplementary Video 1**). Labeled neurons in L6 are visible immediately above the external capsule (EC), where myelinated axons display strong third harmonic generation (THG) signals (**Fig. 2a,b**). The EC features fibrous structure (**Fig. 2b**) extending approximately from 730 to 860 μm below the dura (**Fig. 2a**). GCaMP6s-labeled neurons in the SP layer span from 940 to 1,040 μm below the surface and begin ~80 μm below the EC. Labeled neurons display clear nuclear exclusion and the characteristic honeycomb arrangement of the SP layer (**Fig. 2c**). The distinctly resolved neuron morphology at ~1 mm below the dura shows that 3PM is capable of high-spatial-resolution imaging deep within an intact mouse brain.

We imaged spontaneous activity (without averaging) from the hippocampal neurons at the site shown in **Figure 2c**. We were able to image a population of up to 150 neurons, acquiring fluorescence time traces of neurons of different brightness (**Fig. 2d**). A high signal-to-noise ratio was achieved, which was indicated by the absolute photon counts per neuron per

frame (**Supplementary Figs. 2b** and **5b**). We recorded continuously at a frame rate of 8.49 Hz (256 × 256 pixels/frame) for up to 48 min with a FOV of 200 × 200 μm (**Supplementary Video 2**, 16-min long). The imaging area per unit time reported here is similar to that of calcium imaging using 2PM at shallower imaging depths of the mouse brain tissue[4,6,8]. The average power used was ~50 mW, and no noticeable photobleaching was observed throughout the entire recording session (**Supplementary Figs. 3** and **4**). Higher time resolution for a subset of neurons can be achieved by reducing the FOV or using line scan.

To obtain the activity trace, we integrated the signal from the entire neuron body, which usually consists of more than 100 pixels with the FOV reported. Our results show that the repetition rate of the excitation source is adequate for imaging calcium transients produced by typical GECIs. For structural imaging, longer pixel dwell time or averaging over multiple frames eliminates the impact of the low repetition rate.

Imaging the mouse brain at 1,280 nm with average power up to 120 mW did not result in any noticeable tissue damage[19]. However, the higher intensities required by the nonlinear excitation might induce sample change or damage. Yet, no damage has been observed during functional imaging at L5 at 925 nm with 4- to 5-nJ pulses at the focus[6]. Longer wavelength excitation (~1,300 nm) is less phototoxic[22]. We performed deep cortex and hippocampus imaging by scaling the pulse energy with imaging depth to ensure less than 1.5 nJ at the focal plane. Furthermore, we revisited the same site multiple times many days after the first imaging session, and we successfully recorded neuronal activity from the same population of neurons each time (**Supplementary Figs. 5** and **6**).

We imaged the hippocampal SP layer in a number of mice using ~50-mW average power. Our experimental observation was that hippocampal SP layer imaging will be successful as long as there is insignificant tissue growth under the cranial window, which dramatically increases the amount of laser power necessary for imaging the neurons even for the superficial cortical layers.

An additional feature of 3PM is the intrinsic THG signal[23] generated at various interfaces (e.g., blood vessels and myelinated axons; **Fig. 2**), which provides additional structural information without an exogenous stain.

Reliable turnkey laser systems at 1,300 nm for 3PM are commercially available, and it is relatively straightforward to incorporate such lasers into an existing multiphoton microscope. While the laser systems are more expensive than mode-locked Ti:S lasers for 2PM, it is likely that their cost will decrease and performance improve as the technology matures, which will make long-wavelength 3PM widely available to complement 2PM for deep imaging or imaging densely labeled samples.

3PM can record activity from a large number of neurons with high spatial and temporal resolution deep within scattering brain tissues. Imaging the spontaneous activity in the hippocampal SP layer within an intact mouse brain is just one such demonstration, and the application of our method will enable studies that require noninvasive, high-resolution imaging deep within scattering tissue.

METHODS

Methods, including statements of data availability and any associated accession codes and references, are available in the online version of the paper.

Note: Any Supplementary Information and Source Data files are available in the online version of the paper.

AUTHOR CONTRIBUTIONS
C.X. conceived the study. D.G.O., T.W., M.W., D.D.F., N.G.H. J.C.C.-H., and Y.-T.C. performed the experiments. T.W., D.G.O., and J.R. analyzed the data. C.X. and N.N. supervised the project. J.R. and A.S.T. provided transgenic mice for this study. D.G.O., T.W., and C.X. prepared the manuscript.

COMPETING FINANCIAL INTERESTS
The authors declare no competing financial interests.

Reprints and permissions information is available online at http://www.nature.com/reprints/index.html.

1. Denk, W., Strickler, J.H. & Webb, W.W. *Science* **248**, 73–76 (1990).
2. Zipfel, W.R., Williams, R.M. & Webb, W.W. *Nat. Biotechnol.* **21**, 1369–1377 (2003).
3. Kerr, J.N. & Denk, W. *Nat. Rev. Neurosci.* **9**, 195–205 (2008).
4. Dombeck, D.A., Khabbaz, A.N., Collman, F., Adelman, T.L. & Tank, D.W. *Neuron* **56**, 43–57 (2007).
5. Sato, T.R., Gray, N.W., Mainen, Z.F. & Svoboda, K. *PLoS Biol.* **5**, e189 (2007).
6. Mittmann, W. *et al. Nat. Neurosci.* **14**, 1089–1093 (2011).
7. Dana, H. *et al. eLife* **5**, e12727 (2016).
8. Dombeck, D.A., Harvey, C.D., Tian, L., Looger, L.L. & Tank, D.W. *Nat. Neurosci.* **13**, 1433–1440 (2010).
9. Levene, M.J., Dombeck, D.A., Kasischke, K.A., Molloy, R.P. & Webb, W.W. *J. Neurophysiol.* **91**, 1908–1912 (2004).
10. Jung, J.C. & Schnitzer, M.J. *Opt. Lett.* **28**, 902–904 (2003).
11. Ziv, Y. *et al. Nat. Neurosci.* **16**, 264–266 (2013).
12. Helmchen, F. & Denk, W. *Nat. Methods* **2**, 932–940 (2005).
13. Theer, P. & Denk, W. *J. Opt. Soc. Am. A Opt. Image Sci. Vis.* **23**, 3139–3149 (2006).
14. Theer, P., Hasan, M.T. & Denk, W. *Opt. Lett.* **28**, 1022–1024 (2003).
15. Leray, A., Odin, C., Huguet, E., Amblard, F. & Le Grand, Y. *Opt. Commun.* **272**, 269–278 (2007).
16. Oheim, M., Beaurepaire, E., Chaigneau, E., Mertz, J. & Charpak, S. *J. Neurosci. Methods* **111**, 29–37 (2001).
17. Horton, N.G. *et al. Nat. Photonics* **7**, 205–209 (2013).
18. Andresen, V. *et al. Curr. Opin. Biotechnol.* **20**, 54–62 (2009).
19. Kobat, D. *et al. Opt. Express* **17**, 13354–13364 (2009).
20. Kobat, D., Horton, N.G. & Xu, C. *J. Biomed. Opt.* **16**, 106014 (2011).
21. Chen, T.W. *et al. Nature* **499**, 295–300 (2013).
22. Chen, I.-H., Chu, S.-W., Sun, C.-K., Cheng, P.-C. & Lin, B.-L. *Opt. Quantum Electron.* **34**, 1251–1266 (2002).
23. Squier, J., Muller, M., Brakenhoff, G. & Wilson, K.R. *Opt. Express* **3**, 315–324 (1998).

ONLINE METHODS

Experimental set up. *Excitation source.* The excitation source for 3PM is a noncollinear optical parametric amplifier (NOPA, Spectra Physics) pumped by a one-box regenerative amplifier (Spirit, Spectra Physics). A two-prism (SF11 glass) compressor is used to compensate for the normal dispersion of the optics of the light source and the microscope, including the objective. The NOPA operates at wavelength centered at 1,300 nm and provides an average power of ~500 mW (1,250 nJ per pulse at 400 kHz repetition rate). The pulse duration (measured by second-order interferometric autocorrelation) under the objective is ~55 fs after adjusting the prism compressor. An optical delay line is set up to effectively double the laser repetition rate to 800 kHz. The total optical path length of the delay line is ~3 m, and the two pulses are separated by ~10 ns, which is much longer than the fluorescence lifetime (~1 ns). A half-wave plate (HWP) and a polarizing beamsplitter cube (PBS) are used for power control.

The excitation source for 2PM is a mode-locked Ti:Sapphire laser (Tsunami, Spectra Physics) centered at 920 nm. The output of the Ti:sapphire laser is modulated with an electro-optical modulator (Conoptics, model 350-160), which is capable of sub-μs intensity modulation. The 920-nm beam and 1,300-nm beam are combined by a dichroic mirror (DM), spatially overlapped, and directed to the microscope.

Imaging setup. The images were taken with a custom-built multiphoton microscope with a high-numerical aperture objective (Olympus XLPLN25XWMP2, 25X, NA 1.05). The signal is epicollected through the objective and then reflected by a dichroic beam splitter (FF705-Di01-25 × 36, Semrock) to the detectors. The detection system has two channels: one for green fluorescence signal emitted by the calcium indicator (GCaMP6s) and the other for violet third harmonic generation (THG) signal generated at the interfaces of various structures such as blood vessel walls, neuronal processes, and myelinated axons in the white matter. We use a photomultiplier tube (PMT) with GaAsP photocathode (H7422-40) for the fluorescence signal and an ultra bialkali PMT (R7600-200) for the THG signal. The optical filters for the fluorescence and THG channels are 520/60 (i.e., transmission wavelength centered at 520 nm with a FWHM of 60 nm) band-pass filter (Semrock) and 420/40 band-pass filter (Semrock), respectively. A 488-nm dichroic beam splitter (Di02-R488-25x36, Semrock) is inserted in the signal path at 45° between the two PMTs to separate the THG and fluorescence. The mouse is placed on a motorized stage (M-285, Sutter Instrument Company). A computer running the ScanImage 3.8 (ref. 24) module on MATLAB (MathWorks) software is used to control the stage translation and image acquisition. The PMT current is converted to voltage, amplified and low-pass filtered using a transimpedance amplifier (C9999, Hamamatsu) and an additional 1.9 MHz low-pass filter (Minicircuts, BLP-1.9+). Analog-to-digital conversion was performed by a data acquisition card (NI PCI-6115, National Instruments). For depth measurement, the slightly larger index of refraction in brain tissue (1.35 to 1.43 for the cortex and as high as 1.467 for the white matter), relative to water (~1.33), results in a slight underestimate (5–10%) of the actual imaging depth within the tissue because the imaging depths reported here are the raw axial movement of the objective[18].

Activity recording. For imaging activity, we imaged the neurons continuously using 256 × 256-pixel frame size at 8.49 Hz frame rate for up to 48 min in each imaging session. The average power was ~50 mW under the objective lens. To locate the same imaging site in multiple imaging sessions, we used the surface blood vessel map (imaged in the THG channel) as a guide to navigate the *XY* location. After reaching the same depth as that of the previous imaging sessions, further adjustments in the *XY* position were made according to the tissue morphology (cell, blood vessel, and shadow structure) to ensure that the FOV within the labeled area (total ~400 μm in diameter) was approximately same as before.

Simultaneous two- and three-photon imaging. Simultaneous recording of spontaneous activity with 2PE and 3PE is implemented by time division multiplexing the 920-nm Ti:Sapphire laser beam and 1,300-nm NOPA beam. The 920-nm and 1,300-nm beams are first spatially overlapped to have the same focal position after the objective. The 920-nm beam is switched on only for ~1 μs between two adjacent NOPA pulses by intensity modulation with an electro-optic modulator (EOM). The EOM is driven by a radio frequency signal derived from the NOPA pule train so that the sample is alternatively illuminated either with 920-nm beam for 2PE or 1,300-nm beam for 3PE. By recording the NOPA pulses and the PMT signal at 5 MHz sampling rate (200 ns pixel time), the two- and three-photon excited fluorescence signals are separated in time according to the recorded 1,300 nm laser pulse train with a postprocessing MATLAB script.

Image processing for activity recording. Mechanical drift in the horizontal plane, if any, was corrected with TurboReg plug-in in ImageJ. Regions of interest (ROIs) corresponding to neurons or dendrites were visually identified and selected. Fluorescence intensity traces were low-pass filtered with a hamming window of a time constant of 0.59 s. Baseline of the traces ($F0$) is defined as approximately the lower 20% of each trace during the whole recording time. Intensity traces (F) are normalized according to the formula $(F - F0)/F0$.

Photon counting. To show the absolute signal strength in the unit of photon count rate, pixel values are multiplied by a calibration factor, which is obtained by taking the ratio of the photon count rate with a photon counter (SR400, Stanford Research Systems) and the average pixel value, simultaneously recorded on a uniform fluorescein sample. The calibration factor is further verified by observing the modes of the histogram of an image with a short pixel dwell time such that each pixel typically receives one or zero photon.

Image processing for structural imaging. Images (512 × 512 pixels) taken for structural imaging were processed with a median filter of 1-pixel radius. Images were normalized by stretching the histogram to allow 0.2–0.5% of the pixels to be saturated. 3D reconstruction of the stacks was rendered in Volocity (version 6.3). For the purpose of visualization, the high-resolution images in **Figure 2c**, **Supplementary Figure 2a**, and **Supplementary Figure 5a** were displayed with a gamma correction value of 0.5 (i.e., the square root of the pixel values are displayed) to make the images brighter.

Animal procedures. All animal experimentation and housing procedures were conducted in accordance with Cornell University Institutional Animal Care and Use Committee guidance.

Simultaneous two- and three-photon imaging. Wild-type mice ($N = 2$, 11–12 weeks, male, C57BL/6J, The Jackson Laboratories) retro-orbitally injected with fluorescein (dextran conjugate, 10 kDa,

Invitrogen) were used for SBR measurement on blood vessel. Transgenic mice ($N = 3$, 18–20 weeks old, male, CamKII-tTA/tetO-GCaMP6s) were used for 2PM and 3PM neuron imaging in deep mouse cortex.

Chronic craniotomy. For functional imaging in the mouse cortex, we imaged GCaMP6-labeled neurons in transgenic mice with high labeling density throughout the cortex (CamKII-tTA/tetO-GCaMP6s, 18–20 weeks). Animals were anesthetized using isoflurane (3% in oxygen for induction and 1.5–2% for surgery to maintain a breathing frequency of 1 Hz). Body temperature was kept at 37.5 °C with a feedback-controlled blanket (Harvard Apparatus), and eye ointment was applied. Prior to surgery, glycopyrrolate (0.01 mg/kg body weight), dexamethasone (0.2 mg/kg body weight), and ketoprofen (5 mg/kg body weight) were injected intramuscularly. Dexamethasone and ketoprofen were also administrated in two consecutive days following the surgery. We opened windows of 5 mm in diameter, centered at 2.5 mm lateral and 2 mm caudal from the bregma point over the somatosensory cortex as confirmed by confocal images of postmortem brain slices (**Supplementary Fig. 7**). To reduce tissue growth under the window for chronic imaging, we used a coverslip assembly consisting of a donut-shaped coverslip (inner diameter 4.5 mm, outer diameter 5.5 mm, laser cut by Potomac Photonics) glued concentrically above a 5 mm diameter coverslip (#1 thickness, Electron Microscopy Sciences; optical glue, Norland Optical Adhesive 68). The circular coverslip fit snugly into the open cranial window and was placed directly onto the intact dura. The donut coverslip on the top was glued to the skull (Krazy glue) to keep the inset window pressed against the tissue, displacing as much room for potential tissue growth as possible. The window was further stabilized with dental cement covering the skull and the circular coverslip. In the case of a transgenic mouse, acute imaging happens immediately after the surgery, with the animal kept alive after imaging session. For all mice, chronic imaging happens after at least 5 d after the surgery after tissue inflammation disappears.

Virus injection. For hippocampal imaging, we transfected neurons with AAV virus injection (synapsin promoter, AAV2/1 encapsulation, 4.57×13 gene copies/mL; Penn Vector Core) in wild-type mice ($N = 5$, 8–10 weeks old, males, C57BL/6J, The Jackson Laboratories). The injection took place during the chronic cranial window implantation. The virus was diluted 1:4 in volume with saline and injected using a microinjector (M-10, Narishige) with tapered glass pipette (pipettes, 5-000-2010 Drummond; pipette puller, BV-10 Sutter Instruments) with inner diameter of ~20 µm at the tip. The pipette penetrated normal to the brain surface, and 64 nL virus solution was delivered at depths around 400 µm; 800 µm; 1,200 µm; and 1,600 µm.

No statistical methods were used over a group of animals. No randomization and no blinding was done.

Imaging procedures. At the time of imaging, the mice were anesthetized using isoflurane (1–1.5% in oxygen, maintaining a breathing frequency at 2 Hz) and placed on a heat blanket for maintaining constant body temperature 37.5 °C. Eye ointment was applied, and the animal was place on a 3D motorized stage for navigation under the microscope. For virus-injected mice, we imaged them from the third through the fifth week after the injection. The data shown in **Figure 2** were taken from a mouse imaged on the 28th day after the injection. The same mouse was imaged again 7 days later (**Supplementary Figs. 5** and **6**). Before it was killed for histology, this mouse experienced four imaging sessions beginning the third week after injection.

Histology. At the end of the last imaging session, the animal was deeply anesthetized and transcardially perfused with phosphate buffer saline (PBS, pH 7.4, Sigma-Aldrich) to clear the blood, followed by 4% (w/v) paraformaldehyde (PFA, ThermoFisher Scientific) in PBS. The brains were removed and immersed first in 30% (w/v) sucrose in PBS for 1 d and then in 60% (w/v) sucrose in PBS for 2 d. The brains were frozen in optimal cutting temperature (OCT) compound (Tissue-Tek) and cut in coronal sections at nominal thickness of 100 µm on Microm HM550 cryotome (Thermo Scientific). The brain sections were placed on Superfrost Plus glass slides, mounted with an antifade mountant (ProLong@ Diamond, Life Technologies), covered with a coverslip, and sealed with clear nail polish. The confocal imaging was performed with a commercial microscope (Zeiss LSM 780).

Data availability statement. The data that support the findings of this study are available from the corresponding author upon request.

24. Pologruto, T.A., Sabatini, B.L. & Svoboda, K. *Biomed. Eng. Online* **2**, 13 (2003).